Carbohydrate Research, 160 (1987) 13–28
Elsevier Science Publishers B.V., Amsterdam – Printed in The Netherlands

THE MOLECULAR SIZE AND SHAPE OF XANTHAN, XYLINAN, BRONCHIAL MUCIN, ALGINATE, AND AMYLOSE AS REVEALED BY ELECTRON MICROSCOPY

BJØRN TORGER STOKKE, ARNLJOT ELGSAETER,
Division of Biophysics, University of Trondheim, 7034 Trondheim – NTH (Norway)

GUDMUND SKJÅK-BRÆK, AND OLAV SMIDSRØD
Institute of Marine Biochemistry, University of Trondheim, 7034 Trondheim – NTH (Norway)

(Received March 11th, 1986, accepted for publication, July 18th, 1986)

ABSTRACT

Electron microscopy of some selected, vacuum-dried and rotary-shadowed, polyelectrolytic polysaccharides and glycoproteins adsorbed to mica indicates that this technique can yield reliable information about polymer conformation for chains with persistence lengths q exceeding about 10 nm. Statistical analyses of the local polymer tangent-direction yield q = 150 nm for double-stranded xanthan, q = 60 nm for single-stranded xanthan, q = 45 nm for xylinan, q = 16 nm for alginate (90% β-D-mannuronic acid), and q = 15 nm for human-bronchial mucin. These values are all in adequate agreement with values of q obtained by using other techniques. Amylose, on the other hand, appears as non-randomly aligned chains. The observed contour lengths of amylose indicate a mass per unit length of 1440 dalton/nm, consistent with a pseudo-helical conformation.

INTRODUCTION

Direct electron-microscopic (EM) visibilization of long, flexible macromolecules is potentially a very powerful approach to studying contour length, extension, and flexibility of such molecules. However, the technique has often been viewed with sceptisism, because of the pitfalls associated, in particular, with the specimen preparation of extended, flexible macromolecules. Early electron-micrographs of negatively stained, isolated human erythrocyte spectrin[1,2] are classical examples of some of the problems that may be encountered on using this technique to study flexible polymers. The compact globular structures seen in these early negative-stain studies have later been shown to be preparation artifacts. A slightly different negative-staining procedure, as well as heavy metal replication after vacuum-[3] or freeze-drying[4] of spectrin adsorbed to mica surfaces reveal a floppy, two-stranded structure, in agreement with data from solution studies[5–7] However, the extent to which information about biopolymer flexibility is preserved

0008-6215/87/$ 03 50

in general, after vacuum-drying from glycerol-containing aqueous solution, remains to be established.

In this study, we analyze the conformation of xanthan, xylinan, alginate, human-bronchial mucin, and amylose vacuum-dried from glycerol-containing, aqueous solutions, and replicated by using rotary Pt-shadowing at low angle[8]. The conformation of the macromolecules was analyzed according to Frontali and coworkers[9]. By analyzing the local variation in the tangent direction of the chain, this method yields quantitative estimates of the persistence length, q. The method can be applied to mono- as well as poly-, disperse samples.

We have studied several water-soluble polymers by using this technique. (*1*) Xanthan is an extracellular polysaccharide produced by the Gram-negative bacterium *Xanthomonas campestris*. Its primary structure is based on a pentasaccharide repeat unit consisting of two (1→4)-linked β-D-glucosyl residues in the main chain and a trisaccharide side-chain on alternate D-glucosyl residues[10]. The side chain is frequently substituted with pyruvic acetal on the terminal D-mannose in the side chain, and with acetate on the D-mannose residue adjacent to the main chain. The degree of pyruvic acetal and acetate substitution depends on fermentation conditions and post-fermentation processing. (*2*) Xylinan is an extracellular polysaccharide produced by a cellulose-negative mutant of *Acetobacter xylinum*[11]. It is probably made up of a hexasaccharide repeat unit with a trisaccharide unit in the main chain, and another trisaccharide unit linked to every third saccharide in the backbone[12]. Each hexasaccharide unit carries a negative charge, due to the presence of a glucuronic acid residue. (*3*) Mucin is a glycoprotein which is primarily responsible for the viscoelastic properties of mucous secretions. The mucin used in this study was isolated from sputum from patients with chronic obstructive bronchitis[13]. Mucin is a glycoprotein consisting of a polypeptide backbone with charged carbohydrate side-chains comprised of 2–15 monosaccharides, giving the molecule a bottle-brush-like appearance at low ionic strength. (*4*) Alginates constitute a family of polysaccharides which account for most of the intercellular substance in brown algae, and is used in the industry mainly as a viscosifier, a metal-binding agent, and a gel-former. The alginates are composed of (1→4)-linked residues of β-D-mannuronic and α-L-guluronic acid, varying both in relative amount and sequence along the chain[14,15]. (*5*) Amylose is a polysaccharide made up of (1→4)-linked α-D-glucosyl residues. The conformation of amylose in solution has been modelled as a random coil, but statistical-mechanical calculations indicate that the local propagation of the chains occurs with a preferred tendency for a helical conformation[16,17].

THEORY

Electron micrographs of elongated biopolymers can provide information about contour lengths (L_c), persistence length (q), and end-to-end distance (l_e). If the mass per unit length, M_L, is known, electron microscopy can also be used to

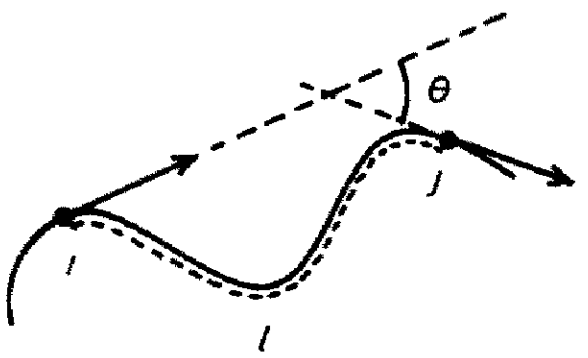

Fig. 1 The difference in tangent direction between two points, i and j, separated a distance l along the polymer contour, is given by angle θ Theory predicts that $\langle\theta\rangle = 0$, $\langle\theta^2\rangle = l/q$ and $\langle\theta^4\rangle/\langle\theta^2\rangle^2 = 3$ when the angle between consecutive, hypothetical links is Gaussian-distributed.

determine molecular weights and molecular-weight distributions. On the other hand, if the molecular weight, M_w, of the sample is known, this method provides a rough estimate of M_L, which, in turn, yields information about secondary structure. The flexibility of the biopolymers can be estimated from the average curvature in two dimensions according to the method of Frontali and coworkers[9],

$$q^{-1} = \langle\theta^2\rangle/l, \tag{1}$$

where q is the persistence length and θ and l are defined in Fig. 1. The Kuhn length, A_m, in the limit of an infinitely long chain is given by $A_m = 2q$. Details of the procedure used to calculate $\langle\theta^2\rangle$ *versus* l is described elsewhere[18]. Integration of the probability density function of θ over L_c for molecules of constant stiffness provides a relation between L_c and l_e with q as the only other parameter[19].

$$\langle l_e^2\rangle = 4qL_c\,\{1 - 2q/L_c\,[1 - \exp(-L_c/2q)]\} \tag{2}$$

Eq. *2* is the well known equation for Porod–Kratky worm-like chains adapted to two dimensions. Eq. *2* provides an estimate of q when L_c and l_e have been determined experimentally. We use the Flory–Fox[20] theory to calculate the root-mean-square end-to-end distance r for random-coil-like molecules in three dimensions.

$$[\eta] = \phi_c\,\langle r^2\rangle^{3/2}/M_w, \tag{3}$$

where $[\eta]$ is the intrinsic viscosity, ϕ_c is a universal constant, $\langle r^2\rangle$ is the mean square end-to-end distance (we use the standard symbol r to denote end-to-end distance in three dimensions, to distinguish it from l_e, which is the end-to-end distance observed in two dimensions using electron microscopy), and M is the molecular weight. Bloomfield and Zimm[21] showed theoretically that the intrinsic viscosity also of extended non-Gaussian chains can be expressed by Eqn. *3*, but then $\phi_c = \phi_c(a)$ is a function of chain flexibility, where a is the exponent in the modified Staudinger equation.

The theory of Yamawaka and Yoshizaki[22] for helical, wormlike chains relates persistence length and intrinsic viscosity.

$$[\eta] = [\eta]_R f(L_c,d,q), \tag{4}$$

where $[\eta]_R$ is the intrinsic viscosity of a stiff rod with length L_c and diameter d (when $L_c/q > 2.278$), or the intrinsic viscosity of a random-coil molecule (when $L_c/q < 2.278$). The mathematical expression for $f(L_c,d,q)$ was given by Yamakawa and Yoshizaki[22]. When L_c and d are known, Eq. *4* can thus be used to estimate q for worm-like macromolecules, provided that the intrinsic viscosity has been determined experimentally.

MATERIALS AND METHODS

Preparation of biopolymer solutions. — Commercially available xanthan (Kelzan XCD, Kelco Inc.) was dissolved (0.3 mg/mL) in 20mM NaCl, pH 7, and stirred overnight at room temperature. The suspension was centrifuged at 90,000*g* for 2 h at 20° (Beckman 50Ti rotor, 35,000 r.p.m.), to remove cell debris and unsolubilized polymer. Xanthan solutions were dialyzed against 5 × 1000 mL of 0.1M ammonium acetate, pH 7, and prepared for electron microscopy as described later. The intrinsic viscosity of xanthan solutions was determined for shear rates from 0.5 s^{-1} to 15 s^{-1}, using a Cartesian diver viscometer[23,24], and the concentration was measured by using the colorometric method of Dubois *et al.*[25]. Xanthan from strain PX061 (kindly provided by Dr. I. W. Sutherland, University of Edinburgh, Scotland) was dissolved overnight in 2mM ammonium acetate at pH 7, ultracentrifuged at 90,000*g* (Beckman 50Ti, 35,000 r.p.m.) for 60 min, and prepared for electron microscopy as described later.

Freeze-dried xylinan (kindly provided by E. Weng, Institute of Marine Biochemistry, University of Trondheim, Norway) was dissolved overnight in 2mM ammonium acetate, pH 7, ultracentrifuged at 90,000*g* for 60 min, and prepared for electron microscopy as described later.

The mucin was isolated from sputum from patients with chronic obstructive bronchitis, using a solubilization and fractionation procedure including treatment with 6M urea at pH 12.5, followed by gel-filtration in 6M urea at neutral pH. Details of this procedure are given elsewhere[13]. The fractionated mucin was prepared for electron microscopy as described later.

An alginate sample enriched in β-D-mannuronic acid (M >90%) was extracted from the intracellular medulla of *Ascophyllum nodosum* receptacles, and further fractionated by precipitation with calcium ions[14]. The alginate sample was converted into the tetramethylammonium (Me_4N^+) salt by dialysis against 0.05M Me_4NCl for 48 h, and then, exhaustively, against distilled water, and freeze-dried. The freeze-dried sample, dissolved in distilled water, was adjusted to pH 7 overnight, and prepared for electron microscopy as described subsequently

Amylose was kindly provided by Dr. D. A. Brant, University of California, Irvine. The sample used in the present study was synthesized enzymically, and carboxymethyl-derivatized (d.s. = 0.08). The sample had the following properties[26]

at 25° in 50mM NaCl: $M_w = 3.89 \times 10^5$ (light-scattering), $R_g = 23$ nm (light-scattering), $M_n = 3.5 \times 10^5$ (osmotic pressure), and $[\eta] = 103$ mL/g. The amylose sample was dissolved in distilled water, the pH adjusted to 8.5, and prepared for electron microscopy as described next.

Electron microscopy. — Biopolymer solutions were mixed with 100% glycerol (Merck Inc., P.A.) and M ammonium acetate, to give a final concentration of 50% of glycerol, 5–30 μg of biopolymer/mL, and the desired ionic strength. This glycerol–biopolymer solution (50 μL) was sprayed on freshly cleaved mica, using a nebulizer constructed according to Tyler and Branton[8], and vacuum-dried for 1 h or more. Vacuum-dried samples were rotary-shadowed with a 0.8-nm thick layer of 95% platinum–5% carbon at an angle of 3–6°, and a 6–8-nm carbon-supporting film at an angle of 90° in the freeze-etch instrument described by Elgsaeter[27]. The elctron micrographs were obtained using a Philips EM 400T electron microscope at electron-optic magnifications of 17,000–60,000×, and final magnification of 100,000–200,000× for quantitative analyses. The contour length, extension, and persistence length of the visibilized macromolecules were determined by digitizing and analyzing the micrographs as described previously[18].

RESULTS AND DISCUSSION

Xanthan. — Fig. 2 shows electron micrographs obtained from representative replica regions of xanthan (Kelzan XCD) vacuum-dried from 0.1M ammonium acetate (A) and 2mM ammonium acetate (B). In the high-salt conditions (A), this xanthan appears as a linear, unbranched polymer with uniform thickness. The end-to-end distance is less than the contour length, and the contour length of this unfractionated sample varies from molecule to molecule. Xanthan sonicated and fractionated by gel-filtration yields molecules with a narrowed contour-length distribution[18]. The calculated mass per unit length, $M_L = 2000$ dalton/nm, corresponds to that of a double-stranded xanthan[18]. Xanthan from the same source occasionally divides into two thinner strands, and, at low ionic strength, this chain-splitting is easily observable (see Fig. 2B). At high ionic strength (see Fig. 2A), the thicker, presumably double-stranded, xanthan is the predominant conformation. Xanthan from strain PX061, in 2mM ammonium acetate, appears only as single-stranded chains, and as aggregated, single strands as the ionic strength is increased[1]. Among xanthan from several sources, the one from strain PX061 was included because it appears as single-stranded structures at conditions (2mM, 20°) where the electrostatic contribution to the persistence length[29] is less than for lower ionic strength which was needed in order to obtain single-stranded structures for other xanthans. The apparent thickness of the single- and double-stranded xanthan, using Pt deposited at an angle of 6° is 4 and 6 nm, respectively. Correcting for the replica thickness, this yields a molecular diameter of ~2 nm for the single- and 4 nm for the double-stranded xanthan.

The distributions of calculated persistence lengths (q) for 72 single- and 74

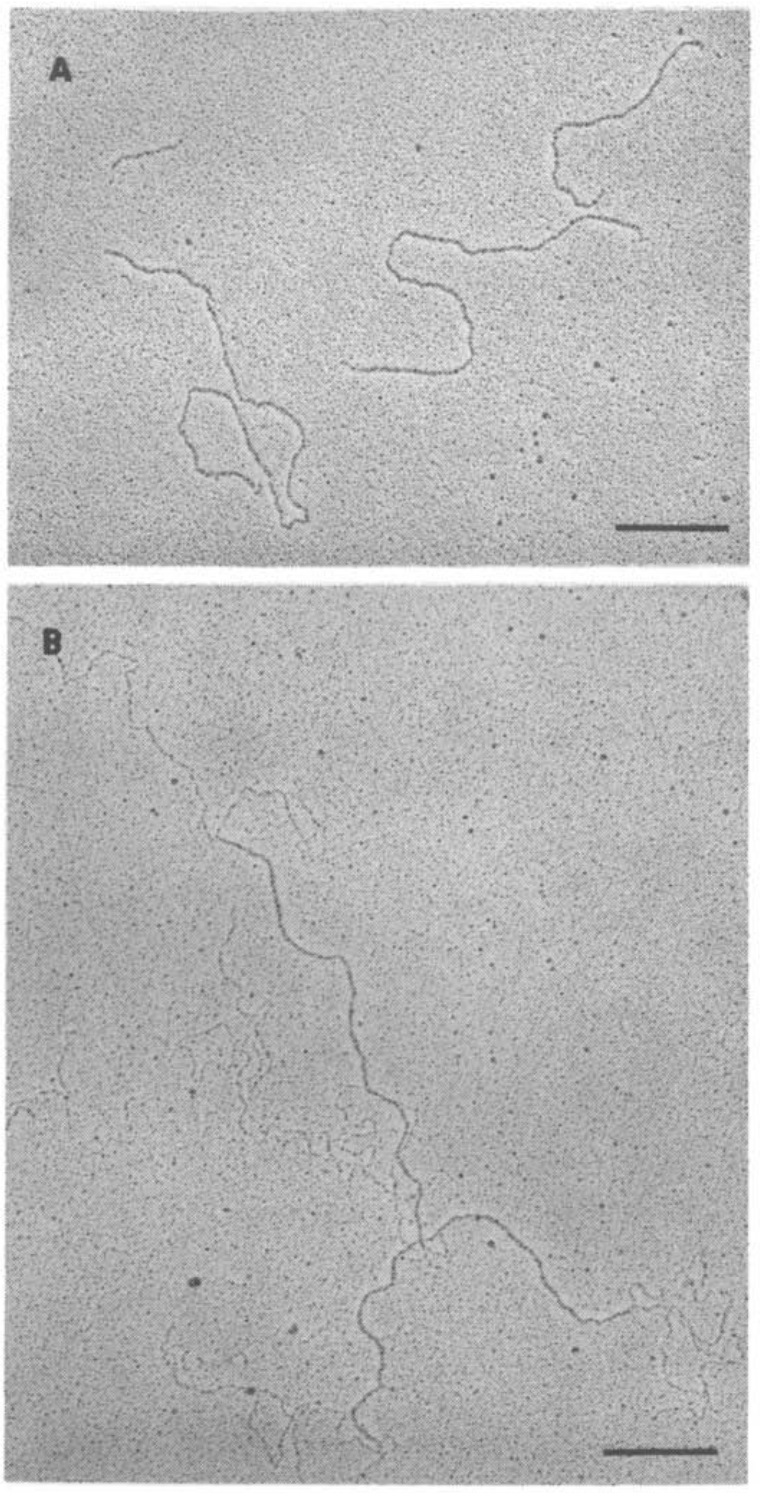

Fig. 2 Representative electron micrographs of xanthan (Kelzan XCD) vacuum-dried from 50% glycerol, 0 1M ammonium acetate, pH 7, (A), and 50% glycerol, 2mM ammonium acetate, pH 7 (B) Rotary replication at 133 μPa with 0 7 nm Pt at an angle of 6°. Bar = 200 nm

double-stranded xanthan molecules yields mean values $q = 58$ nm for single- and $q = 148$ nm for double-stranded xanthan. This is in good agreement with $q = 60$ nm for the single- and $q = 150$ nm for the double-stranded xanthan estimated from $\langle\theta^2\rangle$ *versus* l when $\langle\theta^2\rangle$ was averaged over all the digitized molecules. The assumption that the relative direction of consecutive, hypothetical links exhibits a Gaussian distribution around $\theta = 0$, which corresponds to the rectilinear shape, appears to be fullfilled for the total traced, contour length[18] of 134 μm. The estimated $q = 60$ nm and $q = 150$ nm for the single- and double-stranded xanthan are in good agreement with the values obtained from solution properties. Several estimates of

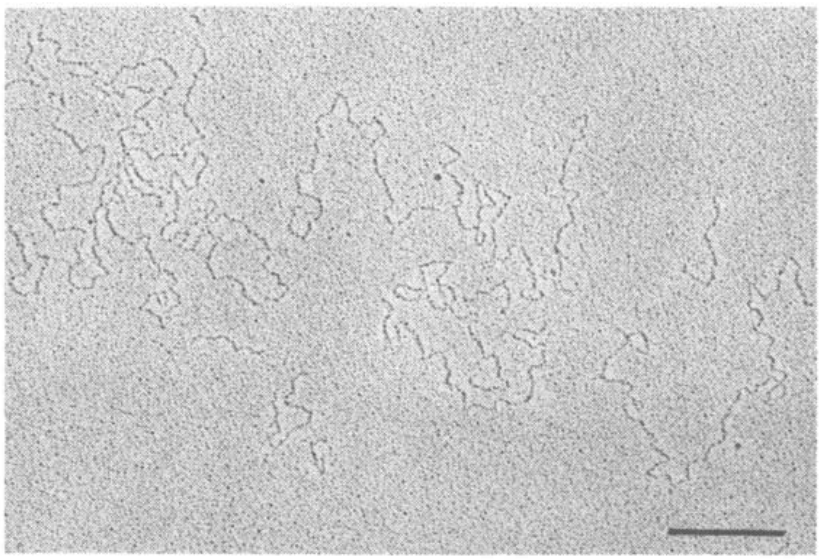

Fig 3 Representative electron micrograph of xylinan vacuum-dried from 50% glycerol, 2mM ammonium acetate, pH 7 Rotary replication at 133 μPa with 0 7 nm Pt at an angle of 5° Bar = 200 nm

q of xanthan have been reported: q = 40–60 nm (based on single-stranded worm-like chain model for intrinsic viscosity[28,29]) q = 75 nm (from shear-rate dependence of the intrinsic voscosity[30]) and q = 100–120 nm (from molecular-weight dependence of both radius of gyration[31] and molecular-weight dependence of the intrinsic viscosity[32,33], modelled as a double-stranded structure). The reasonable agreement between the q values estimated from the electron micrographs of double-stranded xanthan and those reported from hydrodynamic data using the worm-like-coil model, indicates that xanthan adsorbed to mica surfaces and then vacuum-dried and rotary-replicated yields reliable information about xanthan flexibility.

Xylinan. — Fig. 3 shows a representative electron micrograph of xylinan vacuum-dried from 2mM ammonium acetate, 50% of glycerol. Xylinan appears as a linear and unbranched polymer of uniform thickness, and with contour length varying from molecule to molecule. The electron-optic contrast is similar to that of single-stranded xanthan when the shadowing procedure is identical. No branching or chain splitting is observed, which indicates that this polymer is in a single-stranded conformation in 2mM ammonium acetate. The contour length of the present sample is in the range of 300–2000 nm with $\langle L_c \rangle_w$ = 1.200 μm. The chemical structure of the hexasaccharide repeat unit[12] indicates a mass per unit length of 800 dalton/nm in the extended state. The contour lengths observed thus correspond to molecular weights in the range (0.24–1.6) × 10^6 dalton and a weight average M_w of 1.0 × 10^6 dalton. The variance of the change in tangent direction along the biopolymer contour increases linearly with the distance between the points for which θ has been calculated. The slope of a plot of this relationship obtained after averaging over individual molecules yields the distribution of q shown in Fig. 4 (q = 45 ±20 nm s.d., N = 123).

We found that the intrinsic viscosity of xylinan in 2mM ammonium acetate equals 2400 mL/g. Using the theory of Yamakawa and Yoshizaki[22] (Eq. *4*), this

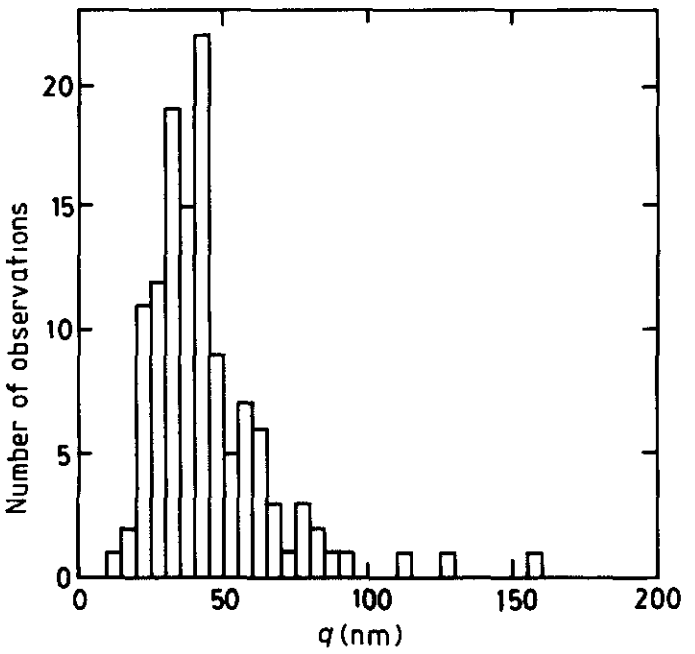

Fig 4 Distribution of persistence lengths estimated from electron micrographs of xylinan vacuum-dried from 50% glycerol, 2mM ammonium acetate Total number of molecules is 123, and the distribution yields $q = 45 \pm 20$ nm (s d)

yields $q = 32$ nm. In this calculation, we used the observed $\langle L_c \rangle_w$, estimated M_w, and assumed a polymer hydrodynamic diameter of ~1.5 nm. This estimate of q is ~70% of that estimated from the electron-microscopic method; however, if M_L of xylinan is assumed equal to 1000 dalton/nm, there is full agreement between q estimated respectively from the intrinsic viscosity and the EM method.

Mucin. — Fig. 5 shows a representative electron micrograph of isolated human-bronchial mucin. Mucin appeared as an unbranched, flexible molecule with uniform thickness. The bottle-brush-like structure is not resolved in the electron micrographs. The carbohydrate side-chains consist of 2–15 monosaccharides, corresponding to a side-chain length of 1–8 nm, which is of the same order as the resolution limit for the replication technique used, but it is noted that the side chains may be folded along the backbone, yielding a smoother overall appearance. Measurements of mucin contour-lengths indicate that the sample is polydisperse[13].

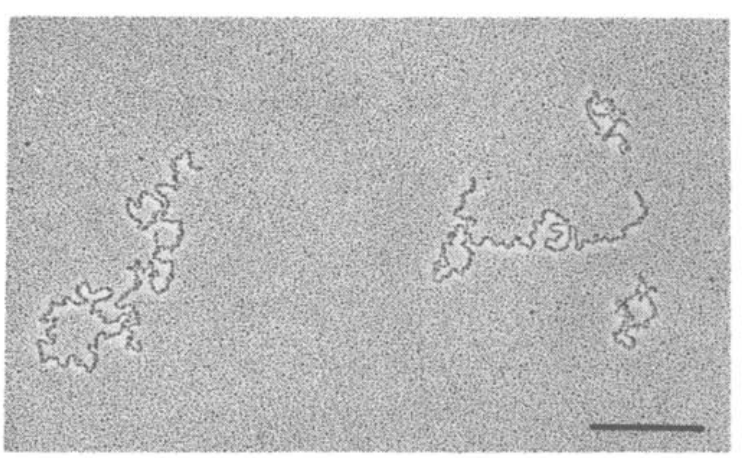

Fig 5 Representative electron micrograph of mucin vacuum-dried from 50% glycerol, ionic strength 3mM, pH 7 Rotary replication at 133 μPa with 0 7 nm Pt at an angle of 5° Bar = 200 nm

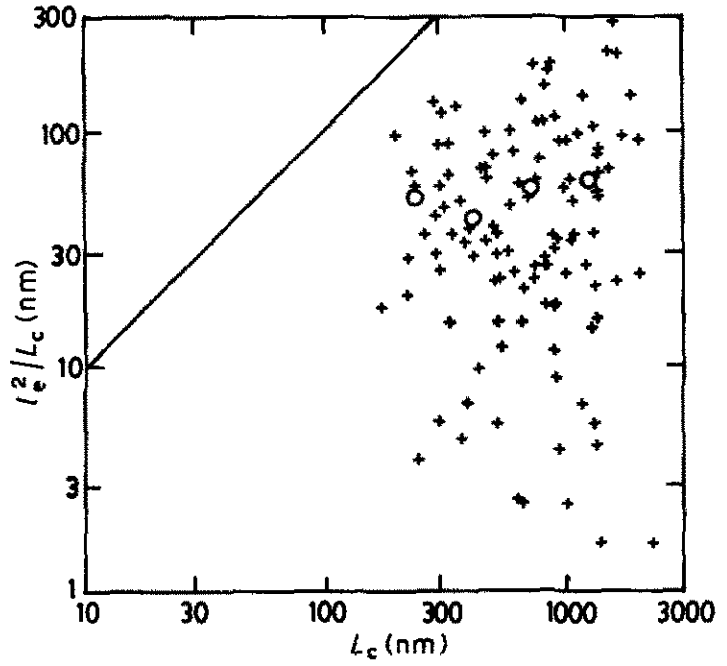

Fig 6. Ratio l_e^2/L_c *versus* L_c for 113 mucin molecules vacuum-dried from 50% glycerol, I = 3mM, pH 7 (+) Average l_e^2/L_c *versus* L_c (O) and stiff-rod limit (——).

The flexible, random-coil-like behavior of mucin is well illustrated by comparing the end-to-end distance with the contour length. Plots of l_e^2/L_c *versus* L_c (see Fig. 6) show that this ratio is only a fraction of what is expected for the stiff-rod conformation. The average of l_e^2/L_c for mucin is almost independent of L_c, as predicted for random-coil-like molecules[34]. Plots of $\langle\theta^2\rangle$ *versus* l, averaged over a total contour-length of 83 μm, yields a persistence length q = 15 nm. However, this value of q corresponds to a much higher stiffness of the mucin chain than the value A_m = 3 nm calculated from the increase in intrinsic viscosity observed when the ionic strength of the solution was decreased, using Smidsrød and Haug's[35] B-parameter[13]. The reason for this discrepancy is not known, but it is noted that the increase in intrinsic viscosity as the ionic strength is reduced may be due to expansion both of the side chains extending from the polypeptide backbone and of the backbone itself. The use of the B-parameter as a measure of chain flexibility may, in the case of mucin, therefore lead to an overestimated chain-flexibility. Furthermore, the correlation between the B-values and Kuhn segment-lengths, A_m, are only valid at infinite ionic strength[35]. The value of A_m obtained at the low ionic strength used in the electron-microscopic study may, therefore, contain a large electrostatic contribution[36], and consequently deviate significantly from the inherent chain-stiffness at infinite ionic strength. The overall extension, as expressed by the end-to-end distance, shows reasonable agreement with the intrinsic-viscosity measurements at low ionic strength when comparison of data is based on the Bloomfield–Zimm[21] equation (Eq. *3*) for semi-flexible chains[13].

Alginate. — Fig. 7 shows a representative electron micrograph of the Me_4N^+ alginate in distilled water. Initially, we used the Na form of the alginate sample, but this yielded electron micrographs where the molecules had very low contrast and could hardly be identified. Replicas of the Me_4N^+ alginate show adequate electron-optic contrast, because the latter counter-ions are bulkier than Na^+. Alginate

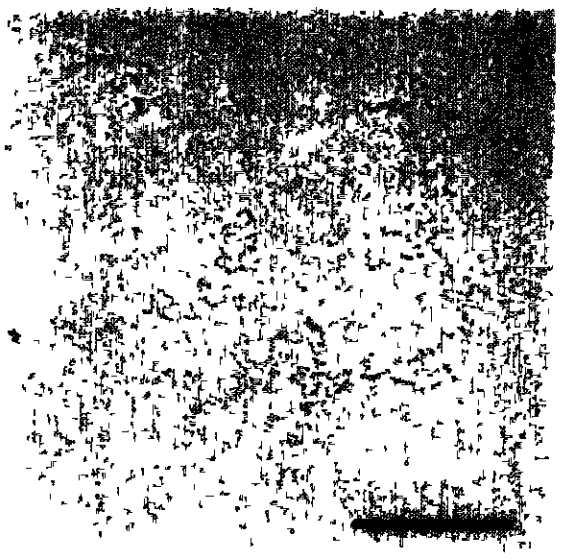

Fig 7 Representative electron micrograph of alginate vacuum-dried from 50% glycerol, pH 7 Rotary replication at 133 μPa with 0 7 nm Pt at an angle of 5° Bar = 200 nm

appears as a linear, unbranched, and flexible structure with contour lengths varying from molecule to molecule, characteristic of a polydisperse, random-coil type of macromolecule. In the quantitative analyses, only molecules where all parts of the chain could be seen distinctly, and therefore be traced easily, were included. This procedure selectively excludes the most convoluted molecules, but the fraction of the untraceable molecules is only ~10%, leading to a possible overestimate of the persistence length of the same relative amount. Fig. 8 shows the distribution of persistence lengths obtained from averaging over individual alginate molecules. The distribution yields $q = 16 \pm 7$ nm (s.d., $N = 67$). This estimate of q is in good agreement with $A_m = 34$ nm in 0.1M NaCl reported by Smidsrød and Haug[37], but corresponds to a significantly higher stiffness than the value $A_m = 10 \pm 6$ nm, independent of ionic strength, reported from light-scattering studies by Strand and

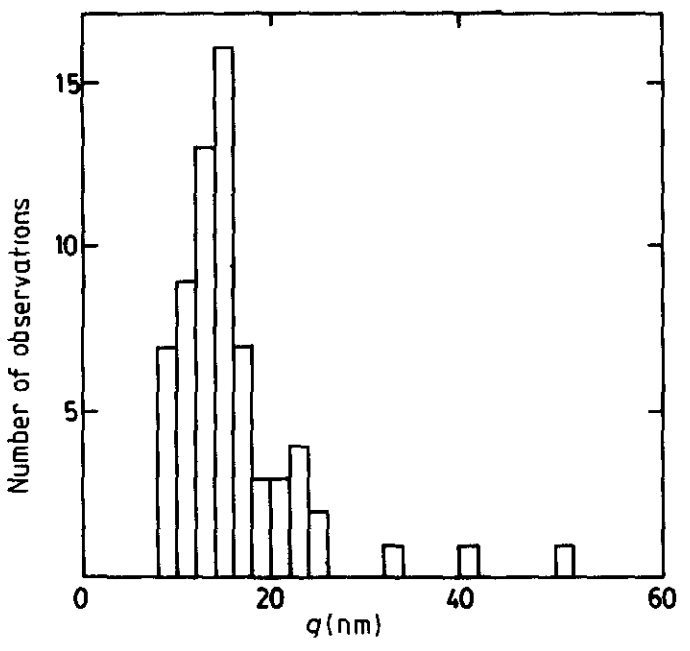

Fig 8 Distribution of persistence lengths estimated from electron micrographs of individual alginate molecules The distribution yields $q = 16 \pm 7$ nm (s d , $N = 67$)

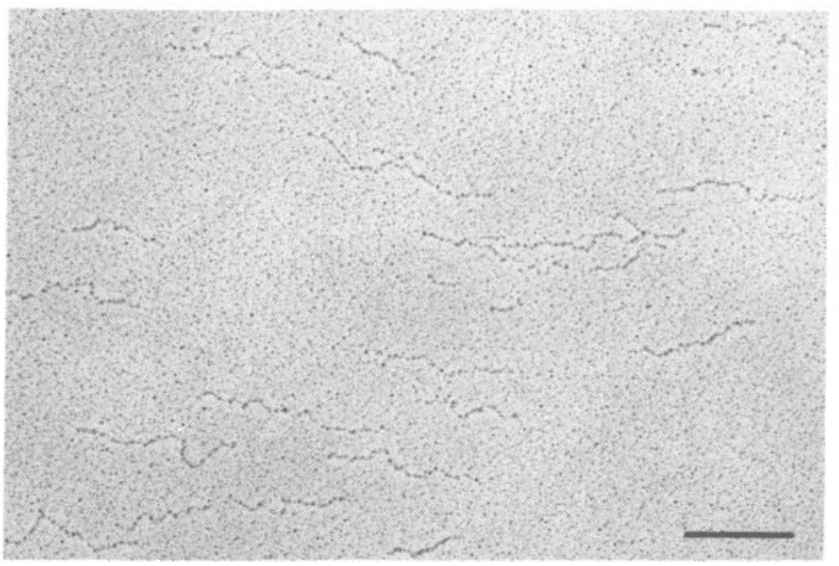

Fig 9 Representative electron micrograph of amylose vacuum-dried from 50% glycerol, pH 8.5 Rotary replication at 133 μPa with 0 7 nm Pt at an angle of 5° Bar = 200 nm

coworkers[38]. However, the present data are not from the same alginate sample, and it is expected that the flexibility of alginate depends on the mannuronic–guluronic acid composition and the sequence of the chain[39]. The present sample contains more D-mannuronic acid than the sample used in the earlier studies of Smidsrød *et al.*[38].

Amylose. — Fig. 9 shows a representative electron-micrograph of the amylose sample used in this study. The amylose molecules appear as structures having uniform thickness, and with contour lengths that are nearly the same for all of the molecules. The amylose molecules are not highly convoluted, as expected from the reported radius of gyration[26], but appear, instead, as consisting of rather stiff segments linked through sharp kinks. Note that most of the amylose molecules on the micrograph appear to be aligned in the same direction. This indicates that solvent flow may have stretched, and lined up, the chains parallel to one another during the vacuum-drying step. The same phenomenon was observed for more than 10 independent, electron-microscopic preparations of amylose, including some preparations where the ionic strength was varied between mM and 300mM ammonium acetate. We have no explanation as to why, in this respect, amylose behaves differently from the other biopolymers discussed in this study. However, we note that of these biopolymers amylose has the lowest charge density, and is the only one having a hollow helix as the preferred conformation[16,17]. The apparent contour-lengths and end-to-end distances were measured for 113 amylose molecules. The contour-length distribution yields $\langle L_c \rangle_w / \langle L_c \rangle_n = 1.05$, which is in excellent agreement with the polydispersity index calculated from the reported number- and weight-average molecular weight[26], $M_w/M_n = 1.1$. We find that $\langle L_c \rangle_w$ equals 270 nm, which yields a mass per unit contour length of 1440 dalton/nm. This is in good agreement with $M_L = 1400$ dalton/nm reported from small-angle, X-ray scattering by Braga and coworkers[26], indicating that amylose also has the pseudo-helical structure after vacuum-drying from glycerol-containing, aqueous solution.

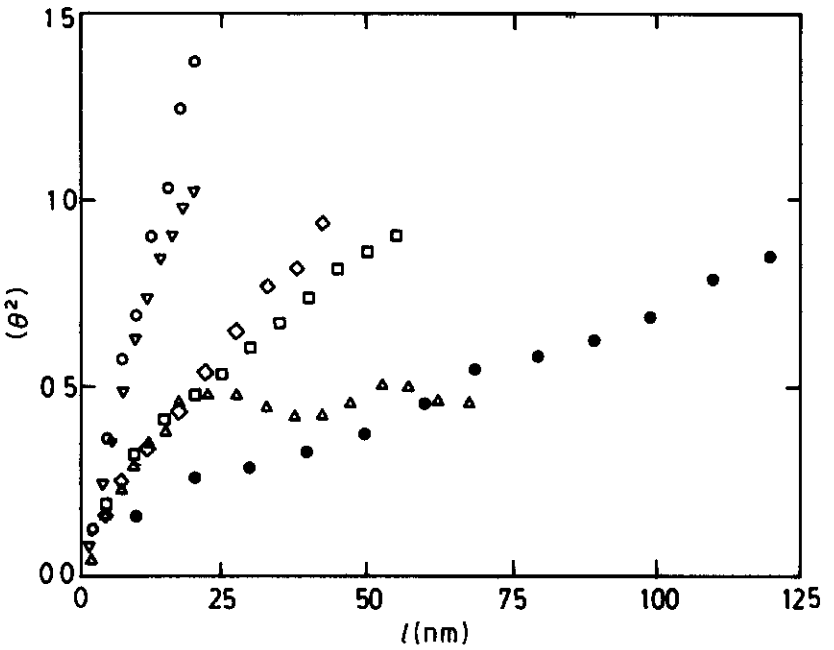

Fig 10 $\langle\theta^2\rangle$ *versus* l for double-stranded xanthan (●), single-stranded xanthan (□), xylinan (◇), mucin (▽), alginate (○), and amylose (△) These macromolecules were vacuum-dried as specified in Figs 2, 3, 5, 7, and 9 For all these polymers, $\langle\theta^2\rangle$ was averaged over a sufficient contour distance that the higher-order moment $\langle\theta^4\rangle/\langle\theta^2\rangle^2$ was equal to 3, and $\langle\theta\rangle$ equal to zero, within experimental error

However, the end-to-end distance, $\langle l_e\rangle_w$ = 240 nm, is much larger than expected from the reported radius of gyration. This is most probably due to the alignment artifacts already discussed.

The variance in the tangent direction along the contour for amylose, $\langle\theta^2\rangle$ *versus* l, increases for l up to 20 nm, but then levels off (see Fig. 10). This, again, is probably an effect of the alignment of the amylose chains during the specimen drying. However, we find that $\langle\theta\rangle$ is close to zero, and $\langle\theta^4\rangle/\langle\theta^2\rangle^2$ is close to 3, for $l/L_c < 0.75$, which indicates that the tangent direction, θ, has Gaussian distribution around $\theta = 0$ (which corresponds to a rectilinear shape). However, because of the non-linear relation between $\langle\theta^2\rangle$ and l (see Fig. 10), the assumptions of the theory of Frontali *et al.*[9] are not satisfied for amylose. The estimate of q based on the initial part of $\langle\theta^2\rangle$ *versus* l, q = 40 nm, is much larger than q = 2.8 nm reported by others[17]

Conformation of vacuum-dried and replicated biopolymers. — During the preparation of flexible biopolymers for electron microscopy (EM), the three-dimensional (3-D) conformation in solution is transformed into an essentially two-dimensional (2-D) conformation. It is therefore not, *a priori,* self-evident that electron micrographs of vacuum-dried and replicated macromolecules contain quantitative information about the polymer-chain flexibility. In their analysis, Frontali and coworkers[9] assumed that the 2-D conformation is the result of permitted chain deformations and not a 2-D projection of the 3-D structure. EM data obtained from the amylose sample indicate that the pseudo-helical nature of this chain is preserved during vacuum-drying and replication. The preparation technique does not deform the pseudohelical structure into the fully extended conformation. Our EM data thus indicate that, in the case of amylose, "permitted

TABLE I

PERSISTENCE LENGTHS (IN nm) FROM ELECTRON MICROSCOPY (E M) AND SOLUTION PROPERTIES

Material	q *(from E M.) (nm)*	q *(from solution properties)*
Double-stranded xanthan	150	100 (ref. 33), 120 (ref. 31)
Single-stranded xanthan	60	40 (ref. 28), 60 (ref. 29)
Xylinan	45	32
Mucin	15	1.5 (ref 13)
Alginate	14	5 ±3 (ref 38), 17 (ref. 37)
Amylose		2 8 (ref. 17)

deformations"[9] involve less energy than is needed to stretch the amylose pseudo-helix itself. On the other hand, the expected random-coil type of behavior of the amylose pseudo-helic does not seem to be preserved during the preparation procedure.

Plots of $\langle\theta^2\rangle$ *versus* l (see Fig. 10) show that $\langle\theta^2\rangle$ increases nearly linearily with l when $\langle\theta^2\rangle < 1$ for all polymers used in the present study, except amylose. The difference in flexibility among the polymers analyzed is well illustrated in this Figure. The persistence length obtained from the initial slope shows reasonable agreement with those reported from solution properties (see Table I). Electron microscopy of vacuum-dried and replicated polymers is expected to yield the most reliable estimate of q for the stiffest polymers, because these chains are least susceptible to shape changes during the vacuum-drying process, due to such factors as solvent flow, surface tension, and increase in ionic strength. The stiffest chains are also the easiest to which to assign an accurate polymer contour, because these chain are the least convoluted. The resolution of the Pt-replication technique used is[40] ~3 nm, which means that, in the biopolymer, details with dimensions less than this are not resolved. The alginate and mucin samples thus appear to represent the lower limit of persistence lengths that can be reliably estimated by electron microscopy of vacuum-dried and replicated polymers.

The persistence length of worm-like coils can easily be estimated when the end-to-end distance and the contour length are known (Eq. *2*). Table II shows

TABLE II

PERSISTENCE LENGTHS (IN nm) CALCULATED USING Eq *2* AND OBSERVED VALUES L_c AND l_e

Material	*Size group* (L_c)			
	30–100	*100–300*	*300–1000*	*1000–3000*
Double-strand xanthan	132	130	76	49
Single-strand xanthan	66	40	45	
Xylinan		30	48	
Mucin		16	14	18
Alginate		10	11	

TABLE III

COMPARISON OF $\langle r^2 \rangle$ CALCULATED FROM $[\eta]$ WITH l_e FROM E M

Material	$[\eta]$ *at (I)*		$\sqrt{\langle r^2 \rangle}$ *Nm* ($\phi_c \times 10^{-23}$)	$\sqrt{\langle l_e^2 \rangle}$ *(nm)*	$\langle L_c \rangle_w$ *(nm)*	M_w $\times 10^{-5}$
	mL/g	*(mM)*				
Double-strand xanthan	7100	(100)	638 (1 5)[a]	561	2608	55
Single-strand xanthan				423	1459	
Xylinan	2400	(2)	267 (1 5)[a]	334	1186	10
Mucin	1500[b]	(10)	205 (2 1)[b]	226	1080	12[b]
Alginate	1100	(100)	144 (2 0)[c]	107	474	5 5
Amylose	103[d]	(50)	54 (2 5)[d]	230	270	3 9[d]

[a]Assumed value [b]Ref 13 [c]Ref 37 [d]Ref 26

persistence lengths for double- and single-stranded xanthan, xylinan, mucin, and alginate, calculated by using this approach. The value of q was estimated for individual molecules (Eq. *2*), and then averaged for different intervals of L_c. For single-stranded xanthan, xylinan, and mucin, there is good agreement between the q value obtained using only L_c and l_e for each molecule (see Table II) and the q value estimated by using the detailed polymer-contour between the starting and ending point of the molecule (see Table I). For double-stranded xanthan, there is adequate agreement between the results of the two methods when L_c <300 nm (see Table II). The reason for the deviation seen for L_c >300 nm is not known. However, the number of molecules used in order to estimate q from Eq. *2* is rather low, whereas the traced contour-length contains data sufficient to satisfy the assumptions in the local tangent direction method. The discrepancy between this q value for alginate (see Table II) and that estimated from the local 2-D conformation may be occasioned because the most convoluted alginate molecules were not included in the analysis, as they could not be reliably traced.

The Flory–Fox theory[20] relates intrinsic viscosity to the root-mean-square end-to-end distance, r (Eq. *3*) We used the observed or reported intrinsic viscosities at one ionic strength in order to estimate $\sqrt{\langle r^2 \rangle}$ using the values for ϕ_c given in Table III. For double-stranded xanthan, M_w was estimated by using the empirical relation between intrinsic viscosities and molecular weights reported by Sato *et al.*[33], for xylinan, M_w was estimated from the observed $\langle L_c \rangle_w$, using an assumed M_L = 800 dalton/nm from the chemical structure; for human-bronchial mucin, M_w was used as estimated previously by Mikkelsen *et al.*[13]; for alginate, M_w was estimated from the Staudinger equation, using coefficients as reported by Smidsrød[15], and, for the amylose sample, the M_w reported by Braga and coworkers[26] was used. Table III shows that there is reasonable agreement between $\sqrt{\langle r^2 \rangle}$ and $\sqrt{\langle l_e^2 \rangle}$ for double-stranded xanthan, xylinan, alginate, and mucin. The discrepancy observed for amylose is probably due to the alignment artifact, as already discussed

In conclusion, this study indicates that vacuum-drying from glycerol-

containing, aqueous solution and Pt-replication on mica of polyelectrolytic carbohydrate polymers with $q > 10$ nm can yield reliable information about polymer size and shape. Analyses of electron micrographs of vacuum-dried and replicated single- and double-stranded xanthan, xylinan, mucin, and alginate all yield persistence lengths that are in adequate agreement with values obtained by using other experimental techniques.

ACKNOWLEDGMENTS

The amylose sample used was kindly provided by Dr. D. A. Brant, University of California, Irvine, U.S.A. Xanthan produced by strain PX061 was kindly provided by Dr. I. W. Sutherland, University of Edinburgh, Scotland, U.K.; this is gratefully acknowledged. We are greatly indebted to Dr. A. Mikkelsen, Division of Biophysics, University of Trondheim, for permission to use his electron micrographs of mucin, and to E. Weng, Institute of Marine Biochemistry, University of Trondheim, for providing xylinan. This work was partly supported by the Exploration and Production Laboratories, The Norwegian State Oil Company (Statoil), Stavanger (grant T. 6399), partly by the Norwegian Council for Science and Industrial Research, and partly by Protan A/S, Drammen.

REFERENCES

1 L G Tilney and P Detmers, *J Cell Biol*, 66 (1975) 508–520
2 Z Kam, R. Josephs, H Eisenberg, and W B Gratzer, *Biochemistry*, 16 (1977) 5568–5572
3 D. M. Shotton, B E Burke, and D. Branton, *J Mol Biol*, 131 (1979) 303–329
4 J E Heuser, *J Mol Biol*, 169 (1983) 155–195
5 A Elgsaeter, *Biochim Biophys. Acta*, 536 (1978) 235–244
6 B T Stokke and A Elgsaeter, *Biochim Biophys Acta*, 640 (1981) 640–645
7 M. H Reich, Z. Kam, H Eisenberg, D Worcester, E Ungewickell, and W B Gratzer, *Biophys. Chem*, 16 (1982) 307–316
8 J M Tyler and D Branton, *J Ultrastruct Res*, 71 (1980) 95–102
9 C Frontali, E Dore, A Ferrauto, E Gratton, A Bettini, M R Pozzan, and E Valdevit, *Biopolymers*, 18 (1979) 1253–1373
10 P E Jansson, L. Kenne, and B Lindberg, *Carbohydr Res*, 45 (1975) 275–282
11 S Valla and J Kjosbakken, *Can J Microbiol*, 27 (1981) 599–603
12 E Weng and O Smidsrød, in preparation
13 A Mikkelsen, B T. Stokke, B E Christensen, and A Elgsaeter, *Biopolymers*, 24 (1985) 1683–1704
14 A Haug, Report No. 30, Norwegian Institute of Seaweed Research, Trondheim, Norway, 1964
15 O Smidsrød, Report No. 34, Norwegian Institute of Seaweed Research, Trondheim, Norway, 1973
16 D A Brant, in J Preiss (Ed), *The Biochemistry of Plants*, Vol. 3, Academic Press, New York, 1980, pp 425–472
17 R C Jordan, D A Brant, and A Cesàro, *Biopolymers*, 17 (1978) 2617–2632
18 B T Stokke, A Elgsaeter, and O Smidsrød, *Int J Biol Macromol*, 8 (1986) 217–225
19 H Hofmann, T Voss, K Kuhn, and J Engel, *J Mol Biol*, 172 (1984) 325–343
20 P J Flory and T G Fox, *J Am Chem Soc*, 73 (1951) 1904–1908
21 V Bloomfield and B Zimm, *J Chem Phys*, 44 (1966) 315–323
22 H Yamakawa and T Yoshizaki, *Macromolecules*, 13 (1980) 633–643
23 M Troll, K A Dill, and B H Zimm, *Macromolecules*, 13 (1980) 436–438
24 B T Stokke, A Mikkelsen, and A Elgsaeter, *Biochim Biophys Acta*, 816 (1985) 102–110

25 M DUBOIS, K A GILLES, J K HAMILTON, P A REBERS, AND F SMITH, *Anal Chem* , 28 (1956) 350–354
26 D BRAGA, E FERRACINI, A FERRERO, A RIPAMONTI, D A BRANT, G S BULGIA, AND A CESÀRO, *Int J Biol Macromol* , 7 (1985) 161–166
27 A ELGSAETER, *J Microsc (Oxford)*, 113 (1978) 83–94
28 G MULLER, J LECOURTIER, G CHAUVETEAU, AND C ALLAIN, *Makromol Chem* , 5 (1984) 203–208
29 G MULLER, M ANRHOURRACHE, J LECOURTIER, AND G CHAUVETEAU, *Int J Biol Macromol* , (1986) in press
30 G M HOLZWARTH, *ACS Symp Ser* , 150 (1981) 15–24
31 T SATO, T NORISYUE, AND H FUJITA, *Polym J* , 16 (1984) 341–350
32 T SATO, S KOJIMA, T NORISYUE, AND H FUJITA, *Polym J* , 16 (1984) 423–429
33 T SATO, T NORISYUE, AND H FUJITA, *Macromolecules*, 17 (1984) 2696–2700
34 L R G TRELOAR, *The Physics of Rubber Elasticity*, 3rd edn , Clarendon Press, Oxford, 1975, pp 59–79 and 101–159
35 O SMIDSRØD AND A HAUG, *Biopolymers*, 10 (1971) 1213–1227
36 T ODIJK, *J Polym Sci , Polym Phys Ed* , 15 (1977) 477–483
37 O SMIDSRØD AND A HAUG, *Acta Chem Scand.*, 22 (1968) 797–810
38 K A STRAND, A BØE, P S DALBERG, T SIKKELAND, AND O SMIDSRØD, *Macromolecules*, 15 (1982) 570–579
39 O SMIDSRØD, R M GLOVER, AND S G WHITTINGTON, *Carbohydr Res* , 27 (1973) 107–118
40 H S SLAYTER, *Ultramicroscopy*, 1 (1976) 341–357